Published in final edited form as:
Angew Chem Int Ed Engl. 2013 February 11; 52(7): . doi:10.1002/anie.201209440.

DNA Micelle Flares for Intracellular mRNA Imaging and Gene Therapy

Tao Chen,
Center for Research at Bio/Nano Interface, Department of Chemistry and Department of Physiology and Functional Genomics, Shands Cancer Center, UF Genetics Institute and McKnight Brain Institute, University of Florida, Gainesville, Florida, 32611-7200

Cuichen Sam Wu,
Center for Research at Bio/Nano Interface, Department of Chemistry and Department of Physiology and Functional Genomics, Shands Cancer Center, UF Genetics Institute and McKnight Brain Institute, University of Florida, Gainesville, Florida, 32611-7200

Elizabeth Jimenez,
Center for Research at Bio/Nano Interface, Department of Chemistry and Department of Physiology and Functional Genomics, Shands Cancer Center, UF Genetics Institute and McKnight Brain Institute, University of Florida, Gainesville, Florida, 32611-7200

Zhi Zhu,
Molecular Science and Biomedicine Laboratory, State Key Laboratory of Chemo/Biosensing and Chemometrics, College of Biology and College of Chemistry and Chemical Engineering, Hunan University, Changsha 410082 (P.R.China)

State Key Laboratory for Physical Chemistry of Solid Surfaces, The Key Laboratory for Chemical Biology of Fujian Province and Department of Chemical Biology College of Chemistry and Chemical Engineering Xiamen University, Xiamen 361005 (China)

Joshua G. Dajac,
Center for Research at Bio/Nano Interface, Department of Chemistry and Department of Physiology and Functional Genomics, Shands Cancer Center, UF Genetics Institute and McKnight Brain Institute, University of Florida, Gainesville, Florida, 32611-7200

Mingxu You,
Center for Research at Bio/Nano Interface, Department of Chemistry and Department of Physiology and Functional Genomics, Shands Cancer Center, UF Genetics Institute and McKnight Brain Institute, University of Florida, Gainesville, Florida, 32611-7200

Da Han,
Center for Research at Bio/Nano Interface, Department of Chemistry and Department of Physiology and Functional Genomics, Shands Cancer Center, UF Genetics Institute and McKnight Brain Institute, University of Florida, Gainesville, Florida, 32611-7200

Xiaobing Zhang, and
Molecular Science and Biomedicine Laboratory, State Key Laboratory of Chemo/Biosensing and Chemometrics, College of Biology and College of Chemistry and Chemical Engineering, Hunan University, Changsha 410082 (P.R.China)

Weihong Tan

Correspondence to: Xiaobing Zhang, xbzhang@hnu.edu.cn; Weihong Tan, tan@chem.ufl.edu.

Supporting information for this article is available on the WWW under http://www.angewandte.org or from the author.

Center for Research at Bio/Nano Interface, Department of Chemistry and Department of Physiology and Functional Genomics, Shands Cancer Center, UF Genetics Institute and McKnight Brain Institute, University of Florida, Gainesville, Florida, 32611-7200

Molecular Science and Biomedicine Laboratory, State Key Laboratory of Chemo/Biosensing and Chemometrics, College of Biology and College of Chemistry and Chemical Engineering, Hunan University, Changsha 410082 (P.R.China)

Xiaobing Zhang: xbzhang@hnu.edu.cn; Weihong Tan: tan@chem.ufl.edu

Abstract

Multifunctional DNA micelles: Molecular beacon micelle flares (MBMFs), based on diacyllipid-molecular beacon conjugate (L-MB) self-assembly, have been developed for combined mRNA detection and gene therapy. The advantages of these micelle flares include easy probe synthesis, efficient cellular uptake, enhanced enzymatic stability, high signal-to-background ratio, excellent target selectivity, and superior biocompatibility. In addition, these probes possess a hydrophobic cavity that can be used for additional hydrophobic agents, holding great promise for constructing an all-in-one nucleic acid probe.

Keywords

DNA micelle; self-assembly; mRNA imaging; gene therapy

The hybridization between a nucleic acid strand and its complementary sequence, one of the strongest and most specific molecular recognition events,[1] has greatly facilitated the development of disease diagnosis and gene therapy. For example, both linear[2] and hairpin nucleic acid probes[3] have been used to visualize and detect specific messenger RNAs (mRNAs) in living cells. Many mRNAs are disease-related and can be used as specific biomarkers to assess the stage of diseases, including cancer. Through molecular engineering, these probes can effectively translate an mRNA binding event into a fluorescence signal change without the need to remove unbound free probes. In addition, most human diseases, even cancer, can be treated with the introduction of genetic materials – plasmid DNAs[4], antisense oligonucleotides[5], small interference RNAs[6], small hairpin RNAs[7], and microRNAs[8] – into somatic tissues. These genetic materials can either enhance gene expression[9] or inhibit the production of deleterious protein, thus making nucleic acid probes excellent candidates for gene therapy[5a]. The advantages of nucleic acid probes lie in the simplicity of their synthesis, the suitability of their modification, and the selectivity of their binding.[1b]

However, their potential has not been fully realized due to the following reasons. First, as negatively charged hydrophilic biomacromolecules, nucleic acid probes cannot freely traverse cell membrane[10], thus requiring additional instruments (such as microinjection and electroporation) or materials (such as transfection reagents including cationic lipids/polymers and nanomaterials) for efficient cellular internalization.[5b] Second, nucleic acid probes can be unstable even after successful cellular delivery because of endogenous nuclease digestion,[11] leading to high false positive signals or decreased therapeutic efficiency. Third, most applications for nucleic acid probes focus on either mRNA detection or gene therapy, while a better strategy that can improve patient outcome is the combining of mRNA imaging[3c, 12] and gene therapy[13] into one biomolecular tool. Through mRNA imaging, real-time spatiotemporal evaluation of nucleic acid probe delivery and target gene expression can be realized non-invasively, providing useful information for assessing therapeutic efficiency, adjusting treatment protocols, and refining probe design.[14] Even though nucleic acid functionalized gold nanoparticles (AuNPs) with efficient cellular

uptake[15] and enhanced enzymatic stability[16] have been developed to solve the first two challenges, they suffer non-negligible cytotoxicity at relatively high concentrations as a result of AuNP incorporation.[17] In addition, the preparation of these probes is very time-consuming, requiring more than 24 hours even after obtaining AuNPs and nucleic acids.[5b] Therefore, an ideal nucleic acid probe should be easy to synthesize, possess self-delivery capability, be highly biocompatible, and be sufficiently stable in cellular environment, while at the same time, performing multiple functions in living cells.

Here we present a sensitive and selective approach for combined mRNA detection and gene therapy using molecular beacon micelle flares (MBMFs). MBMFs are easily prepared by diacyllipid-molecular beacon conjugate (L-MB) self-assembly, not requiring any materials of potential biohazard. Just like pyrotechnic flares that produce brilliant light when activated, MBMFs undergo a significant burst of fluorescence enhancement upon target binding. This hybridization event subsequently induces gene silencing, leading to cancer cell apoptosis. The advantages of MBMFs include easy probe synthesis, efficient cellular uptake, enhanced enzymatic stability, high signal-to-background (S/B) ratio, excellent target selectivity, and superior biocompatibility. In this approach (Scheme 1), L-MBs spontaneously self-assemble into MBMFs with diacyllipid core and MB corona in aqueous solutions due to hydrophobic interactions. The MB part is a DNA sequence composed of a target-recognition loop flanked by two short complementary stem sequences. The formation of the stem-loop (hairpin) structure brings the quencher and fluorophore, which are located at the opposite ends of MB, into close proximity, thus effectively quenching fluorescence (“OFF state”). When hybridized to target mRNA, the MB in MBMFs experience a conformation change that opens the hairpin structure, physically separating the fluorophore from the quencher to allow fluorescence to be emitted upon excitation (“ON” state). In addition, the hybridization of MBMFs to the target mRNA can specifically inhibit gene expression through different mechanisms, including translational arrest by steric hindrance of ribosomal activity and the induction of RNase H endonuclease activity,[18] leading to the suppression of cancer cell growth.

L-MBs with illustrated structure (Figure 1a) were prepared by directly coupling diacyllipid phosphoramidite onto the 5’-end of MBs on a fully automated DNA/RNA synthesizer, purified by reverse-phase high-pressure liquid chromatography (HPLC) (Figure S1a and S1b), and characterized by ESI-MSn (Figure S1c). Diacyllipid phosphoramidite was synthesized through a three-step reaction according to our previously reported procedure.[19] After purification, L-MBs spontaneously form MBMFs in aqueous solution with very low critical micelle concentration (CMC) (below 10 nM, Figure S2), indicating their excellent stability compared to polymer-micelle systems.[20] The formation of MBMFs was further confirmed by both agarose gel electrophoresis (Figure 1b) and dynamic light scattering (DLS) (Figure 1c). MBMFs migrated much slower than MBs without diacyllipid, suggesting the successful formation of larger micelle nanostructures. DLS measurements showed that MBMFs had a diameter of 17.1 nm. After adding synthetic complementary target (cDNA), the diameter increased to 29.4 nm, while incubating MBMFs with synthetic random control (rDNA) resulted in negligible size increase. Detailed size distribution information can be obtained from the Supporting Information (Figure S3). These results indicated that MBMFs maintained target recognition capability after the formation of a micellar structure and that the binding event did not disrupt the structural integrity of the micelle. Consistent results were also obtained from zeta-potential measurements: values of −6.2, −10.8, and −7.1 mV were obtained for MBMFs only, MBMFs treated with cDNA, and MBMFs treated with rDNA, respectively (Figure 1d). Detailed sequence information for all the probes used can be found in Supporting Information (Table S1)

The performance of MBMFs was first evaluated in buffer system. According to fluorescence spectroscopy results, MBMFs were specific to target sequences, with approximately 10-fold signal increase for cDNA which is much higher than previously mentioned AuNP-nucleic acid conjugates[5b, 17, 21], but only minimal enhancement for rDNA (Figure 2a). In addition, MBMFs were able to differentiate between perfectly complementary target and mismatched targets (Figure 2b). The fluorescence signal of MBMFs exhibited dose-dependent increases in response to cDNA concentrations from 0 to 1 μM (Figure 3c and Figure S4) with a wide dynamic range from 0 to 200 nM (Figure 3c, Inset). These results demonstrated that MBMFs could effectively signal the presence of target with excellent selectivity and sensitivity. To compare the stability of MBMFs and MBs towards enzymatic digestion, we incubated each with endonuclease DNase I (1U/mL, significantly greater than what would be found in the cellular environment) and monitored the fluorescence signal increase as a function of time. The results revealed a much slower increase in fluorescence signal for MBMFs compared to MBs, indicating their enhanced stability due to increased resistance to enzymatic digestion (Figure 2d). Similar phenomenon was also observed for MBMFs and MBs in cell lysate (Figure S5).

After testing the feasibility of the MBMF approach with a synthetic target, the ability of MBMFs to permeate cell membrane and detect target mRNA was further investigated. The loop region of L-MBs was designed to be perfectly complementary to *c-raf-1* mRNA, a cancer biomarker and antisense therapeutic target of great significance in cancer diagnostics and theranostics. Noncomplementary MBMFs with similar background signal, but little response to target (Figure S6), were used as control. A549 cells were used to verify the ability of MBMFs to detect intracellular mRNA in the tumor microenvironment. These adenocarcinoma human alveolar basal epithelial cells come from cancerous lung tissue and have a high expression level of *c-raf-1* mRNA.[5a]

In order to obtain optimum results for intracellular detection of *c-raf-1* mRNA, we optimized both probe concentration and incubation time for all cell experiments. A549 cells cultured on coverglass-bottom confocal dishes were incubated with 150, 300, and 600 nM MBMFs, respectively, and then imaged under a confocal laser scanning microscope. Increasing fluorescence signal was observed for cells treated with increasing concentration of MBMFs (Figure S7). We noticed that cells treated with 150 nM MBMFs did not generate sufficient fluorescence signal to illuminate *c-raf-1* mRNA, while cells treated with 600 nM MBMFs resulted in poor S/B ratio. Therefore, the optimal probe concentration was 300 nM, which had the best combined fluorescence signal and S/B ratio. We also studied the influence of incubation time on fluorescence signal by incubating A549 cells with 300 nM MBMFs for 2 and 4 h, respectively. Because similar fluorescence intensity was observed for both times (data not shown), 2 h was chosen as the assay time for the remaining cell experiments. In addition, the co-localization assay demonstrated that most fluorescence came from the cytoplasm, instead of endosomes or lysosomes (Figure S8), indicating that the signal was caused by the specific binding of MBMFs to *c-raf-1* mRNA.

Under optimized conditions, confocal laser scanning microscopy results revealed that A549 cells treated with MBMFs (Figure 3a) displayed much more fluorescence than the population treated with noncomplementary control (Figure 3b) and MBs (Figure 3c), demonstrating the selectivity of the system and the need of diacyllipid for efficient self-delivery, respectively. In comparison, normal bronchial epithelial cell line HBE135 from healthy lung tissue, which expresses significantly less *c-raf-1* mRNA,[22] displayed very low fluorescence (Figure S9). We also used flow cytometry to collect the fluorescence data for cells treated with MBMFs. Compared to confocal laser scanning microscopy, which allows imaging of only a small number of cells, flow cytometry can analyze thousands of cells per second, generating a quantifiable statistical average for a large population of cells, while

eliminating cell-to-cell variation and experimental artifacts. The flow cytometry results were in excellent agreement with confocal imaging: 2.61 and 1.08 times signal enhancement were observed for A549 and HBE135 cells, respectively (Figure 3b). Thus, while MBMFs work for synthetic target detection in buffer system, these results also demonstrate that MBMFs are feasible for intracellular mRNA detection in living cells. In addition, the MBMF approach can also differentiate cell lines with distinct mRNA expression levels, such as the cancerous and normal cells used here.

Before they can be used for gene therapy, MBMFs must first hybridize with mRNA. The probe acts either by providing a translation block, preventing translation from the targeted mRNA, or by forming a DNA/RNA hybrid with the target mRNA, causing it to be degraded by enzyme RNase H.[18] Using these mechanisms, the MBMFs can be used for imaging guided gene therapy.[14a] In this effort, we used *Raf* genes which code for serine threonine-specific protein kinases that play pivotal regulatory roles in the development and maintenance of certain human malignancies. Substantial evidence supports the theory that antisense oligonucleotides targeted against *c-raf-1* kinase can specifically inhibit *c-raf-1* mRNA expression and tumor progression through aforementioned mechanisms when properly delivered. Therefore, we also tested the antiproliferative effect of MBMFs on cancer cells. Since gene therapy based on antisense oligonucleotides requires a long treatment period, phosphorothioate MBMFs (S-MBMFs) were used to avoid any potential nuclease digestion in living cells that would diminish therapeutic efficiency. Experiment results showed that this backbone modification didn't significantly affect the performance of S-MBMFs compared to MBMFs since they had similar background fluorescence without target and maximal fluorescence with excess target or non-target (Figure S10). In addition, S-MBMFs had comparable CMC (below 20 nM, Figure S11) as MBMFs (below 10 nM, Figure S2). According to the cytotoxicity assay (Figure 4), A549 cell growth was negligibly influenced by the treatment of cells with noncomplementary S-MBMFs, indicating the superior biocompatibility of our system compared to some metal nanoparticle systems.[17] However, their treatment with S-MBMFs resulted in marked inhibition of cell proliferation in a dose-dependent manner, suggesting that MBMFs can be applied as an antisense therapy for cancer cells with high expression level of *c-raf-1* mRNA.

In summary, we have presented a novel nanoprobe based on molecular assembly that can be used for combined mRNA detection and gene therapy. Current advantages for this approach include easy probe synthesis, efficient cellular uptake, enhanced enzymatic stability, high S/B ratio, excellent target selectivity, and superior biocompatibility. Instead of incorporating potentially biohazardous materials for efficient nucleic acid probe delivery, easy molecular engineering of MBs with diacyllipid provided the resulting MBMFs with new properties that MBs do not have, such as self-delivery capability and enhanced intracellular stability. In addition to their use in the context of mRNA imaging and gene therapy, MBMFs possess a hydrophobic cavity for additional hydrophobic materials, such as magnetic contrast agents and anticancer drugs, showing great promise for constructing an all-in-one nucleic acid probe capable of imaging, diagnosis, and therapy at the same time.

Supplementary Material

Refer to Web version on PubMed Central for supplementary material.

Acknowledgments

This work is supported by grants awarded by the National Institutes of Health (GM066137 and GM079359), and by the National Key Scientific Program of China (2011CB911000), the Foundation for Innovative Research Groups of NSFC (Grant 21221003), China National Instrumentation Program 2011YQ03012412. The authors thank Dr. Haipeng Liu and Dr. Ruowen Wang for their help on diacyllipid phosphoramidite synthesis, Dr. Craig G.

Moneypenny and Dr. Neal A. Benson for their technical assistance with confocal laser scanning microscopy and flow cytometry, and Dr. Kathryn Williams for her critical comments on the preparation of this manuscript.

References

1. a) Tyagi S, Kramer FR. Nat. Biotech. 1996; 14:303–308.b) Wang K, Tang Z, Yang CJ, Kim Y, Fang X, Li W, Wu Y, Medley CD, Cao Z, Li J, Colon P, Lin H, Tan W. Angew. Chem. Int. Ed. 2009; 48:856–870.
2. a) Molenaar C, Marras SA, Slats JCM, Truffert JC, Lemaitre M, Raap AK, Dirks RW, Tanke HJ. Nucleic Acids Res. 2001; 29:e89. [PubMed: 11522845] b) Okabe K, Harada Y, Zhang J, Tadakuma H, Tani T, Funatsu T. Nucleic Acids Res. 2011; 39:e20. [PubMed: 21106497]
3. a) Tyagi S. Nat. Meth. 2009; 6:331–338.b) Monroy-Contreras R, Vaca L. J. Nucleic Acids. 2011 Article ID 741723. c) Tan W, Wang K, Drake TJ. Curr. Opin. Chem. Biol. 2004; 8:547–553. [PubMed: 15450499]
4. Horton HM, Anderson D, Hernandez P, Barnhart KM, Norman JA, Parker SE. PNAS. 1999; 96:1553–1558. [PubMed: 9990062]
5. a) Monia BP, Johnston JF, Geiger T, Muller M, Fabbro D. Nat. Med. 1996; 2:668–675. [PubMed: 8640558] b) Seferos DS, Giljohann DA, Hill HD, Prigodich AE, Mirkin CA. J. Am. Chem. Soc. 2007; 129:15477–15479. [PubMed: 18034495]
6. Giljohann DA, Seferos DS, Prigodich AE, Patel PC, Mirkin CA. J. Am. Chem. Soc. 2009; 131:2072–2073. [PubMed: 19170493]
7. Paddison PJ, Caudy AA, Bernstein E, Hannon GJ, Conklin DS. Genes Dev. 2002; 16:948–958. [PubMed: 11959843]
8. Hao L, Patel PC, Alhasan AH, Giljohann DA, Mirkin CA. Small. 2011; 7:3158–3162. [PubMed: 21922667]
9. Wang J, Zhang PC, Mao HQ, Leong KW. Gene Ther. 2002; 9:1254–1261. [PubMed: 12215893]
10. Du FS, Wang Y, Zhang R, Li ZC. Soft Matter. 2010; 6:835–848.
11. Wu Y, Yang CJ, Moroz LL, Tan W. Anal. Chem. 2008; 80:3025–3028. [PubMed: 18321137]
12. a) Peng XH, Cao ZH, Xia JT, Carlson GW, Lewis MM, Wood WC, Yang L. Cancer Res. 2005; 65:1909–1917. [PubMed: 15753390] b) Liu X, Tan W. Anal. Chem. 1999; 71:5054–5059. [PubMed: 10575961]
13. a) Askari FK, McDonnell WM. N. Engl. J. Med. 1996; 334:316–318. [PubMed: 8532029] b) Smith RA, Miller TM, Yamanaka K, Monia BP, Condon TP, Hung G, Lobsiger CS, Ward CM, McAlonis-Downes M, Wei H, Wancewicz EV, Bennett CF, Cleveland DW. J. Clin. Inves. 2006; 116:2290–2296.
14. a) Liu G, Swierczewska M, Lee S, Chen X. Nano Today. 2010; 5:524–539. [PubMed: 22473061] b) Wang H, Chen X. Expert Opin. on Drug Delivery. 2009; 6:745–768.
15. Patel PC, Giljohann DA, Daniel WL, Zheng D, Prigodich AE, Mirkin CA. Bioconjugate Chem. 2010; 21:2250–2256.
16. Seferos DS, Prigodich AE, Giljohann DA, Patel PC, Mirkin CA. Nano Lett. 2008; 9:308–311. [PubMed: 19099465]
17. Jayagopal A, Halfpenny KC, Perez JW, Wright DW. J. Am. Chem. Soc. 2010; 132:9789–9796. [PubMed: 20586450]
18. Elsabahy M, Nazarali A, Foldvari M. Curr. Drug Deliv. 2011; 8:235–244. [PubMed: 21291381]
19. a) Liu H, Zhu Z, Kang H, Wu Y, Sefan K, Tan W. Chemistry – Eur. J. 2010; 16:3791–3797.b) Wu Y, Sefah K, Liu H, Wang R, Tan W. PNAS. 2010; 107:5–10. [PubMed: 20080797]
20. Lukyanov AN, Gao Z, Mazzola L, Torchilin VP. Pharm. Res. 2002; 19:1424–1429. [PubMed: 12425458]
21. Li N, Chang C, Pan W, Tang B. Angew. Chem. Int. Ed. 2012; 51:7426–7430.
22. Rapp, UR.; Storm, SM.; Cleveland, JL. Modern Trends in Human Leukemia VII. Vol. Vol. 36. Berlin Heidelberg: Springer-Verlag; 1987. p. 450-459.

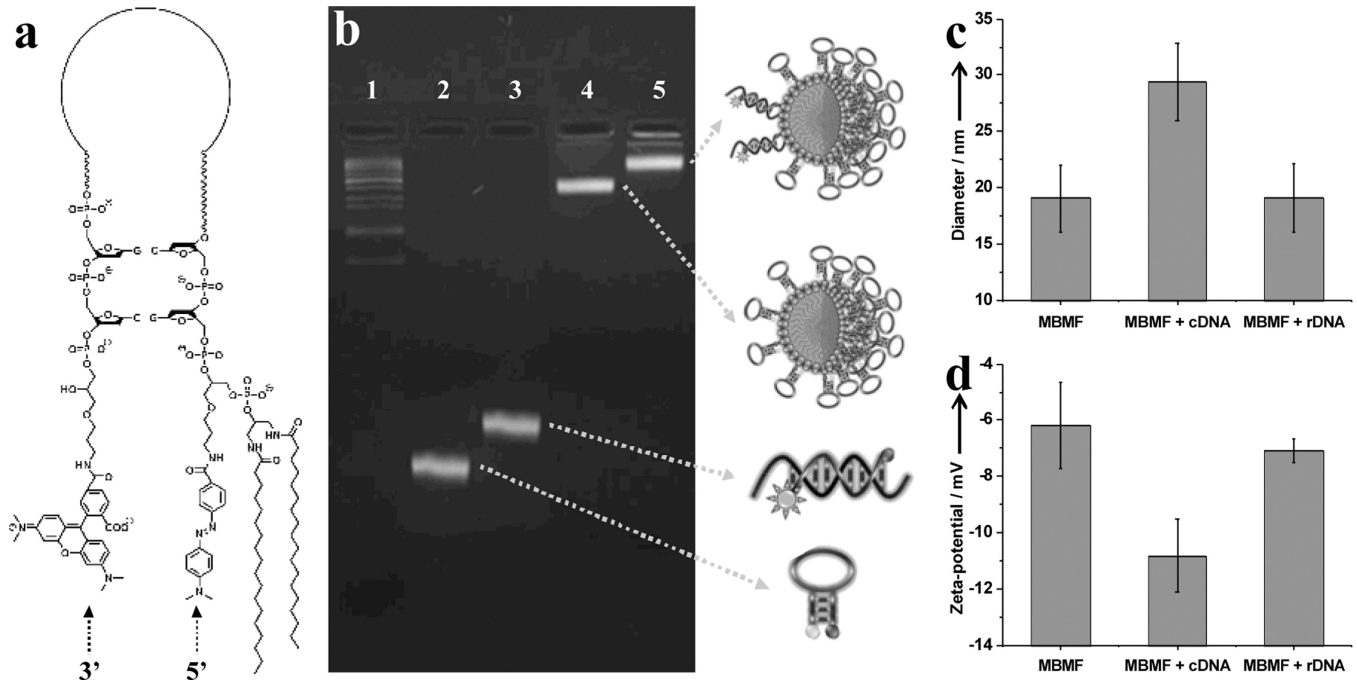

Figure 1.

Characterization of MBMFs. (a) Structure of MBMFs. Note: Not all the bases are shown. (b) Agarose gel electrophoresis of DNA marker (lane 1), MBs (lane 2), MBs with synthetic complementary target (cDNA) (lane 3), MBMFs (lane 4), and MBMFs with cDNA (lane 5). (c) DLS and (e) zeta-potential measurements of MBMFs, MBMFs with cDNA, and MBMFs with synthetic noncomplementary target (rDNA).

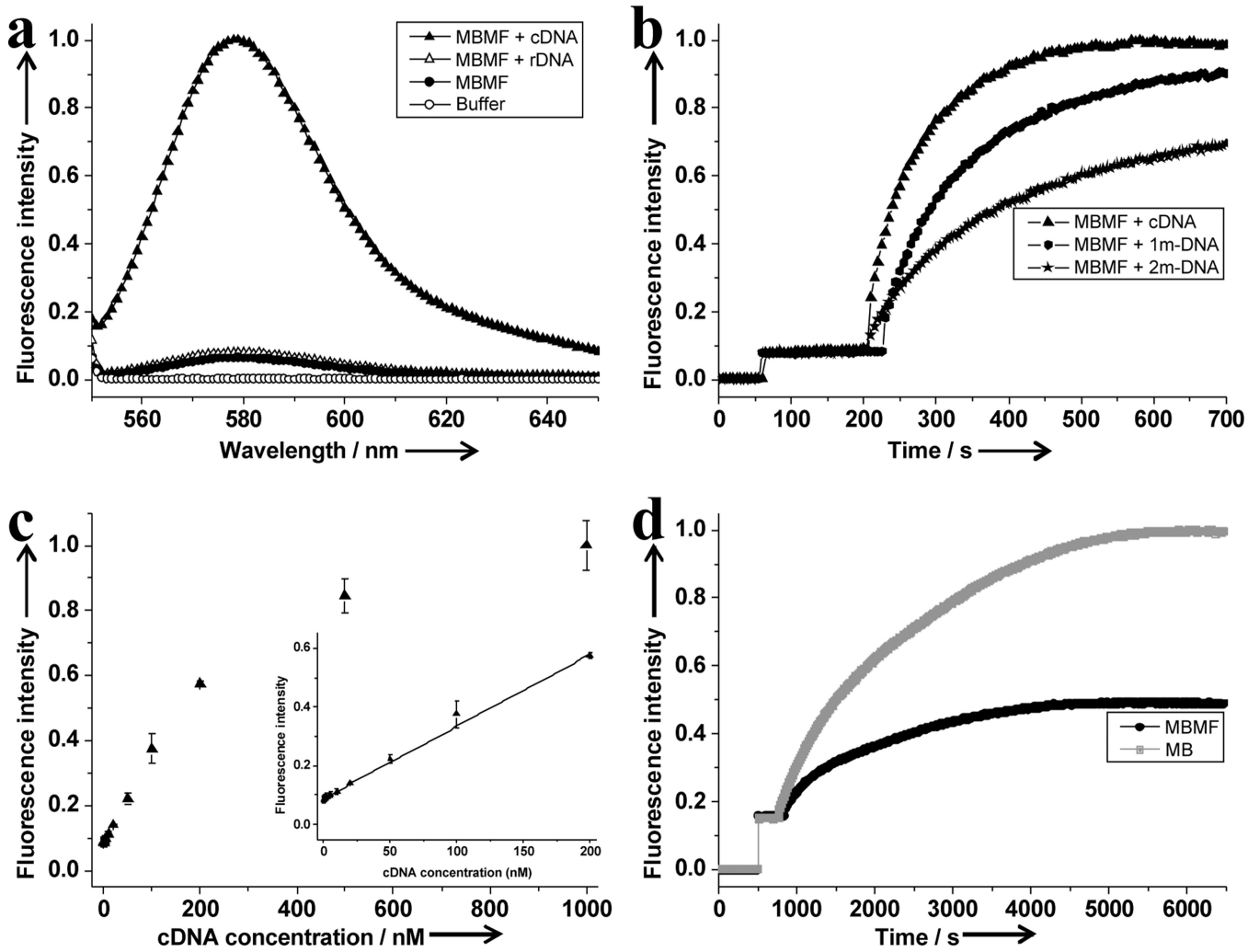

Figure 2.

Performance evaluation of MBMFs in buffer system. (a) Fluorescence emission spectroscopy of MBMFs treated with cDNA and rDNA. (b) Fluorescence kinetics spectroscopy of MBMFs treated with cDNA, synthetic 1-base mismatch target (1m-DNA), and synthetic 2-base mismatch target (2m-DNA). (c) Response of MBMFs to cDNA with concentrations ranging from 0 to 1 μM. Inset: Response of MBMFs to cDNA with concentrations ranging from 0 to 200 nM with an excellent linear relationship. (d) Fluorescence kinetics spectroscopy of MBMFs and MBs treated with DNase I.

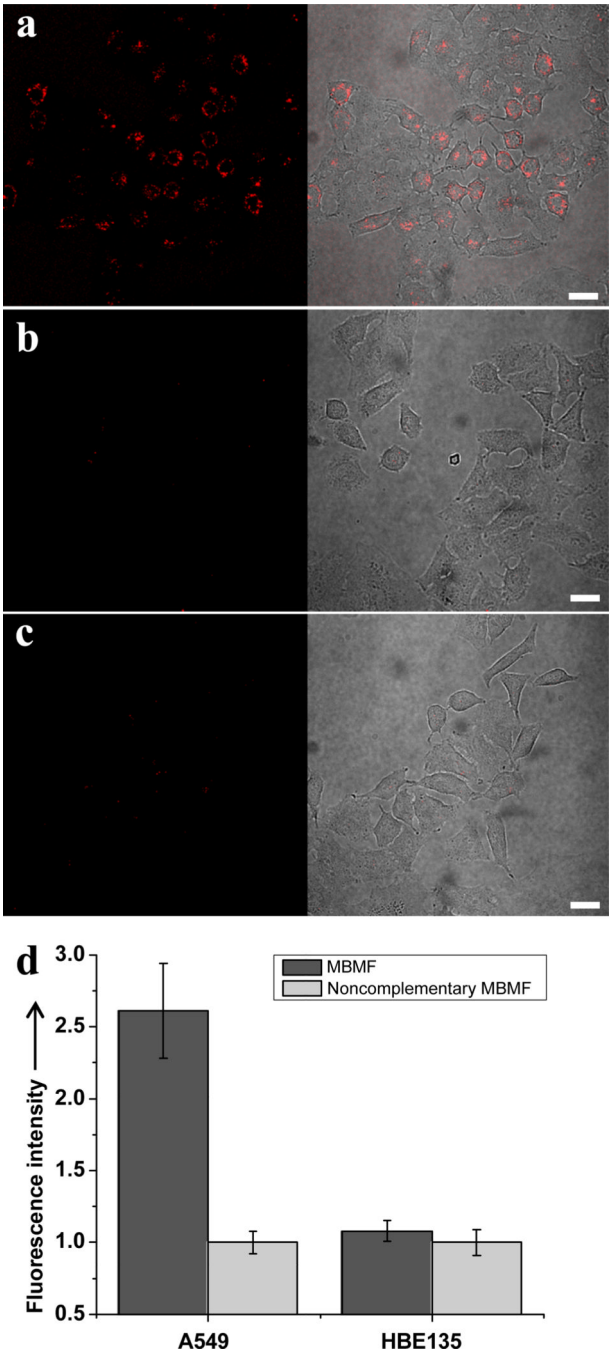

Figure 3.

Capability investigation of MBMFs in living cells. Confocal laser scanning microscopy images of A549 cells treated with 300 nM (a) MBMFs, (b) non-complementary MBMFs, and (c) MBs. Left panels are TAMRA fluorescence pseudo-colored red, and right panels are the overlay of TAMRA fluorescence and bright field image. Scale bars: 20 μm. (d) Flow cytometry results of A549 and HBE135 cells treated with 300 nM MBMFs and non-complementary MBMFs.

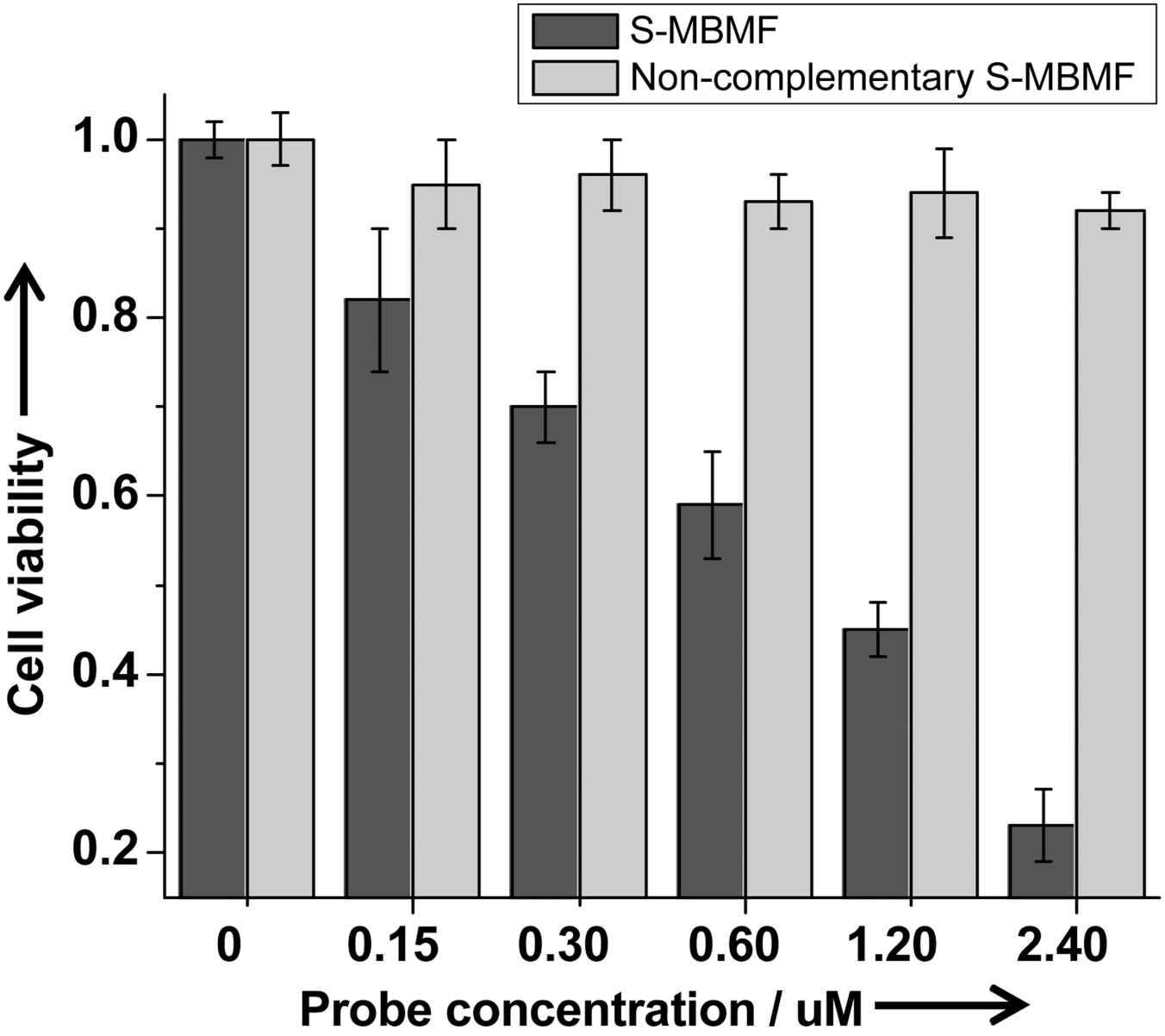

Figure 4.
Cytotoxicity assay of A549 cells treated with S-MBMFs and non-complementary S-MBMFs.

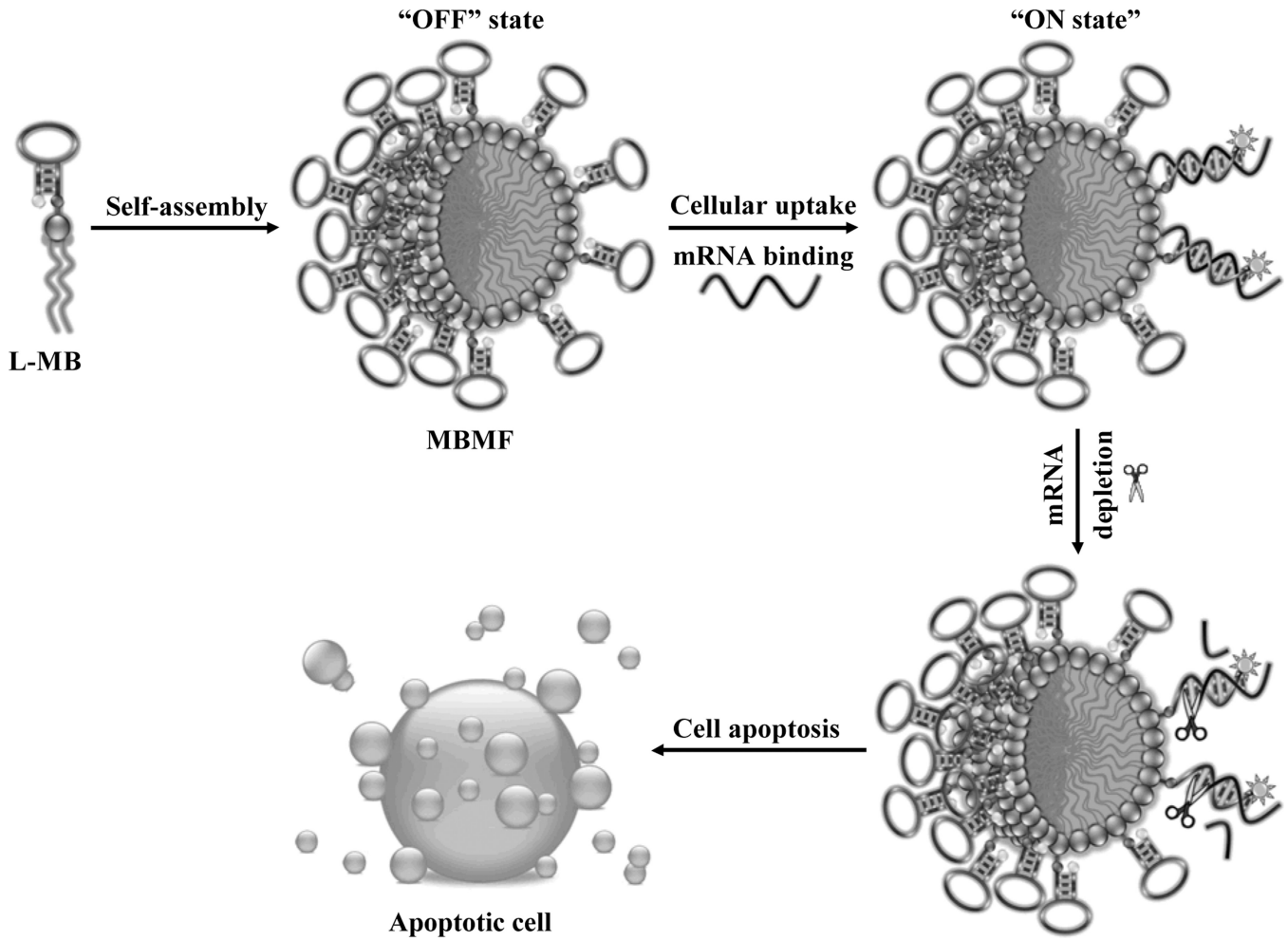

Scheme 1.

Schematic illustration of molecular beacon micelle flares (MBMFs) for intracellular mRNA detection and gene therapy. Diacyllipid-molecular beacon conjugates (L-MBs) self-assemble into MBMFs and enter living cells. Before meeting their target mRNA, the fluorophore and the quencher in MBMFs are in close proximity ("OFF state"). However, hybridization between the loop region and target mRNA separates the fluorophore and the quencher, producing a fluorescence signal ("ON state") and heteroduplex for RNase H action. Note: In order to maintain the aesthetics of the scheme, not all MBs are shown on the MBMF.